NASA TECHNICAL MEMORANDUM NASA TM-77373

FLOW MECHANISM AND EXPERIMENTAL INVESTIGATION OF A ROTATING STALL IN TRANSONIC COMPRESSORS

Lu Yajun and Zhang Shunlin

Translation of "Kuayin yaqiji xuanzhuan shisu jili ji shiyan yanjiu," Acta Aeronautica et Astronautica Sinica, Vol. 3, June 1982, pp. 61-71

(NASA-TM-77373) FLOW MECHANISM AND EXPERIMENTAL INVESTIGATION OF A ROTATING STALL IN TRANSONIC COMPRESSORS (National Aeronautics and Space Administration) 21 p HC A02/MF A01 CSCL 21E G3/02

N84-15122

Unclas 14503

NATIONAL AERONAUTICS AND SPACE ADMINISTRATION
WASHINGTON, D.C. 20546 DECEMBER 1983

ORIGINAL PAGE IS
OF POOR QUALITY

STANDARD TITLE PAGE

1. Report No.	2. Government Accession No.	3. Recipient's Catalog No.
NASA TM-77373		

4. Title and Subtitle	5. Report Date
FLOW MECHANISM AND EXPERIMENTAL INVESTIGATION OF A ROTATING STALL IN TRANSONIC COMPRESSORS	December 1983
	6. Performing Organization Code
7. Author(s)	8. Performing Organization Report No.
Lu Yajun and Zhang Shunlin, Beijing Aeronautical Engineering College	10. Work Unit No.
9. Performing Organization Name and Address	11. Contract or Grant No. NASW-3541
Leo Kanner Associates Redwood City, California 94063	13. Type of Report and Period Covered: Translation
12. Sponsoring Agency Name and Address	14. Sponsoring Agency Code
National Aeronautics and Space Administration, Washington, D.C. 20546	

15. Supplementary Notes

Translation of "Kuayin yaqiji xuanzhuan shisu jili ji shiyan yanjiu," Acta Aeronautica et Astronautica Sinica, Vol. 3, June 1982, pp. 61-71

(A82-45193)

16. Abstract

The flow characteristics of the rotating stall in compressors is studied, and a flow model is developed along with a theoretical calculation method based on vortex theory. A detailed theoretical calculation is completed for a two-dimensional flow field in a transonic rotor in a rotating stall, and the result is in good agreement with experimental findings. The oscillograms of time-varying stall characteristic parameters recorded for the onset, growth, and cessation processes of rotating stall are analyzed, and some new flow phenomena deserving of further investigation are discovered. These include serious separation of individual blades, often preceding the onset of rotating stall in compressors with very small blade-camber angles, and periodical variation of the circumferential width of the stall cell with time, accompanied by periodical oscillation of the width of the stall cell in the radial direction of the blade. The circumferential and radial oscillation frequencies are the same.

17. Key Words (Selected by Author(s))	18. Distribution Statement
	Unclassified-Unlimited

19. Security Classif. (of this report)	20. Security Classif. (of this page)	21. No. of Pages	22.
Unclassified	Unclassified		

FOREWORD

/61

Due to the complexity of the physical phenomenon of a rotating stall in compressors, many factors including some random ones can affect the stall. Therefore, for many years researchers sought to determine the quantitative relationship between the geometrical and gas-dynamic parameters of compressors on the one hand, and the characteristic parameters on the other, in stall conditions, but no satisfactory results have been attained. Recently, with the increasing enhancement in characteristics of axial-flow type compressors, the type of unsteady flow phenomenon like a rotating stall exerts a more serious effect and destructive role on compressor properties. Frequently, the stall causes breaking of compressor blades, and even major incidents like the destruction of the compressor and the death of its operator. Therefore, the study of this type of unsteady flow phenomenon (in gas dynamics) like the rotating stall is still one of the important topics in the field of aeronautical science and technology.

This paper conducts analysis and study of the properties of gas flow in rotating stall conditions; by utilizing the vortex theory, the vortex system flow model and the calculation method of the flow field are established in the rotating stall conditions. Based on this calculation method, relatively detailed theoretical calculations are conducted on a low-speed rotor and a transonic rotor. The calculated flow field matches quite well with the measured flow field. This explains the soundness of the flow model and the calculation method of the flow field. In addition, the paper conducts analysis and study of the time-varying oscillogram of the stall property parameters recorded during the onset, growth and cessation processes of the rotating stall phenomenon of a transonic rotor. Several new flow phenomena worth attention in research were discovered, as follows: (1) the phenomenon of turbulent separation (serious separation of a single blade) occurred before the rotating stall condition; (2) in the varying process of

the stall flow state, the periodic variation with time of the circumferential width of the seapration zone with the simultaneous periodic variation of the width of the separation zone along the blade height direction.

FLOW MECHANISM AND EXPERIMENTAL INVESTIGATION OF A ROTATING STALL IN TRANSONIC COMPRESSORS

Lu Yajun and Zhang Shunlin
Beijing Aeronautical Engineering College

I. Establishment of Physical Model of Gas Flow and its Calculation Formulas in Stall Condition /62*

In order to better realize and understand the flow properties and the affected factors in rotating stall conditions, it is required to establish a flow model to reveal this type of flow phenomenon. We know from some experimental data in sudden-change rotating stall conditions that vortex motions exist in the upper and lower streams of the blade row in this stall condition. Therefore, obviously the use of the vortex theory to establish a flow model in such working condition can better reveal the property of this type of flow phenomenon than other means. In an axial flow type compressor, once the phenomenon of rotating stall occurs, the axial symmetry of the entire flow field is destroyed. If the coordinate system is fixed in a rotating separation zone, the entire flow field is then divided into two circulating flow zones with entirely different properties. Within the main flow zone outside of the separation zone, fundamentally the circulating flow and momentum of gas current are the same as in a certain steady-state condition. Within the low-speed gas flow in a separation zone, the intense separation of the gas current will considerably reduce the circulating flow momentum. Since there is a relative motion between the blade row and the separation zone, each blade of the blade row will enter and leave this separation zone in sequence. When each blade completes one cycle of entering and leaving the separation zone, the circulating flow momentum of the gas on the blade will vary once in back-and-forth fashion. This variation is the source producing

---

* Numbers in the margin indicate pagination in the foreign text.

the periodic oscillation force on the blade when the blade enters the separation zone from the main flow zone via one side of the boundary in the separation zone; the circulating flow momentum on the blade varies from a large to a small value. Therefore, a vortex flowing from the blade tail to the lower stream of the blade row has the same circulating momentum and direction on the blade in the main flow zone. This phenomenon is similar to the situation during an aircraft takeoff; simultaneously as the air current forms an adhering vortex on the aircraft wings, a takeoff vortex must remain on the ground. Since blades of a blade row enter and leave the separation zone continuously in sequence from two sides of the boundary of the separation zone, two steady vortex streets remain on two sides of the boundary of the separation zone. If consideration should be given to the adhering effect, the intensity of two vortex streets downstream from the blade row will gradually be weakened and dissipated. In this paper, two finite-length vortex streets of equal intensities are used to consider calibration of this adhering effect in the flow model. The relative motion between the low-speed flow (or even the reverse flow) in the separation zone and the incoming flow in front of the blade row enables the rotating motion to take place in the upper stream of the blade row (the upper stream of the vortex street). The shape of the vortex street is related to the size of the separation zone and the magnitude of the gas flow speed. In order to simplify the flow model and complexity of the calculation, a method is used where the lower-stream vortex street extends toward the upper stream by a certain distance while considering the effect of the existence of the vortex in the upper stream. Figure 1 presents a vortex flow model /63
established in the paper. From the flow model of the vortex system, the following flow field calculation formula can be deduced:

$$\vec{W} = \vec{W}_1 + \vec{W}_2 + \vec{W}_3 + \vec{W}_\infty$$

In the formula,

$$W_{1x} = + \frac{\Gamma}{2t} \frac{\mathrm{sh}(2\pi y/t)}{\mathrm{ch}(2\pi y/t) - \cos(2\pi x/t)} \qquad (1)$$

$$W_{1y} = - \frac{\Gamma}{2t} \frac{\sin(2\pi x/t)}{\mathrm{ch}(2\pi y/t) - \cos(2\pi x/t)}$$

In the equation, Γ is the intensity of the point vortex, and t is the grid distance of the blade row.

The subscripts u and a indicate, respectively, the components along the direction of the x and y axes. Similar situations are applied in the following:

$$W_{2u} = \sum_{i=1}^{l_{20}/t} W_{2u_i} \tag{2}$$

$$W_{2a} = \sum_{i=1}^{l_{30}/t} W_{2a_i}$$

In the equations,

$$W_{2u_i} = -\frac{\Gamma}{2L} \frac{\operatorname{sh}(2\pi y/L)}{\operatorname{ch}(2\pi y/L) - \cos(2\pi \eta_i/L)}$$

$$W_{2a_i} = +\frac{\Gamma}{2L} \frac{\sin(2\pi y/L)}{\operatorname{ch}(2\pi y/L) - \cos(2\pi \eta_i/L)}$$

$$\eta_i = x$$

c is the value of the x coordinate of a certain blade in the separation zone; L is the circumferential length of the circular blade grid; and ℓ_{30} is the nominal width of the separation zone.

$$W_{3u} = U_3 \cos(\pi + \delta) + V_3 \cos \delta \tag{3}$$

$$W_{3a} = U_3 \sin(\pi - \delta) + V_3 \sin \delta$$

In the equations,

$$U_3 = \frac{|\gamma|}{2\pi} \sum_{n=-\infty}^{+\infty} (\theta_{hn} - \theta_{wn})$$

$$V_3 = \frac{|\gamma|}{2\pi} \sum_{n=-\infty}^{+\infty} \left(\frac{\sin\alpha''_{hn} \sin\alpha'_{wn}}{\sin\alpha'_{hn} \sin\alpha''_{wn}} \right)$$

δ is the bearing angle of the vortex street; γ is the intensity of the vortex street.

θ_{hn}, θ_{wn}, α'_{hn}, α'_{wn}, α''_{hn}, and α''_{wn} are, respectively, the geometrical parameters in the vortex system model in Fig. 1.

$$W_{mu} = v \sin\delta - \frac{\sum_{i=1}^{n_u}(W_{1u}+W_{2u}+W_{3u})_i}{n_u} \tag{4}$$

$$W_{ma} = -\left[C_a + \frac{\sum_{i=1}^{n_a}(W_{1a}+W_{2a}+W_{3a})_i}{n_a}\right]$$

In the equations, v is the gas flow speed in the main flow zone; /64 C_a is the mean speed value of the axial-direction inlet gas in the rotor; n_a is the number of calculation points at the calculation cross-section; and n_u is the number of calculation points at the calculation cross-section outside of the separation zone.

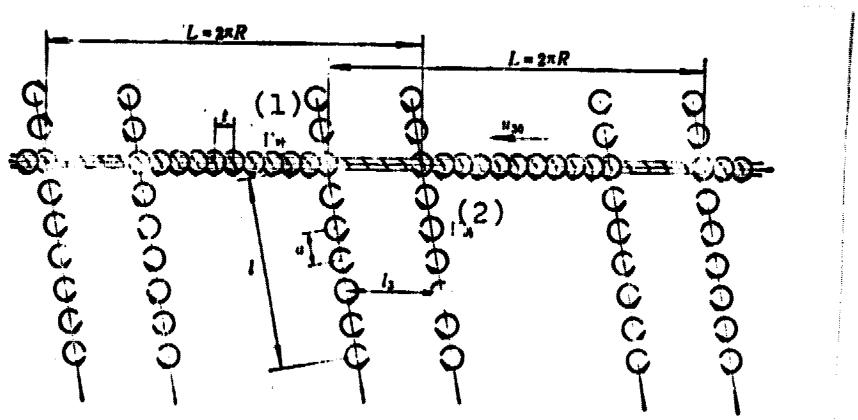

Fig. 1. A flow model of a vortex system in a rotating stall condition.
Key: (1) Blade; (2) Rotor.

Refer to Literature [1] for the detailed calculation method related to the two-dimensional flow field. Figure 2 shows the flow speed field of a transonic rotor calculated using the above method. In order to prove the correctness and soundness of the model, Fig. 3

presents the measured speed field. By comparing flow speed fields and analysis, we can see that this model is sound.

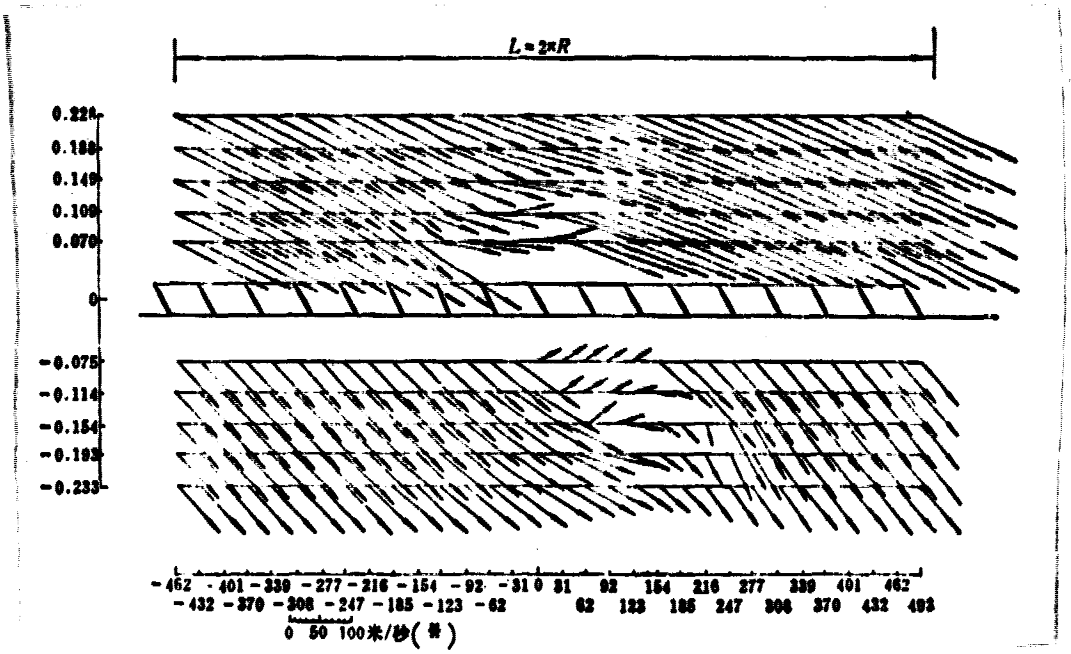

Fig. 2. The calculated flow field in a transonic rotor in a rotating stall at n=13000 rpm with mass flow coefficient $\bar{C}_a$=0.263.
Key: (*) Meters per second.

II. Experimental Equipment and Test Instruments /65

This test stand is a single-and-double stage compressor test equipment. The rated power of the test stand is about 2000 hp; its rated rpm is 22,000 rpm; and its test flow range is 0 to 25 kilograms per second. For the transonic compressor used for experimentation and study, the designed rotating speed is 22,000 rpm; its designed flow is 13.6 kilograms per second; its pressure ratio between stages under designed conditions is about 1.6; and the relative Mach numbers at blade tip and blade root are, respectively, 1.4 and 0.9.

ORIGINAL PAGE IS
OF POOR QUALITY

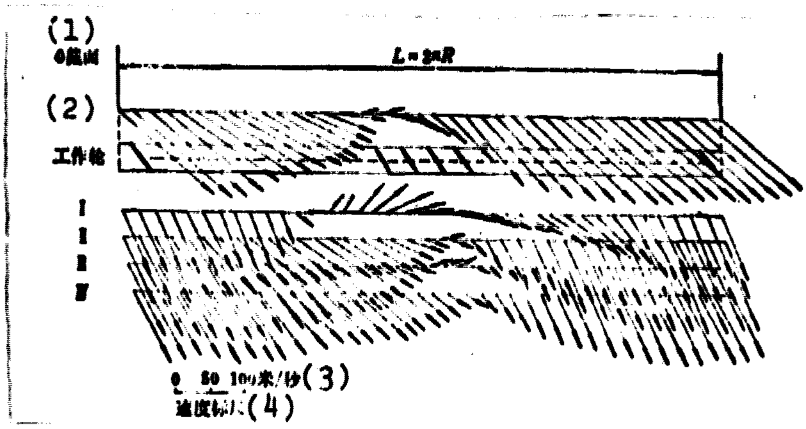

Fig. 3. The measured flow field in a transonic rotor in a rotating stall at n=13000 rpm with mass flow coefficient $\bar{C}_a$=0.263.
Key: (1) Cross-section 0; (2) Working wheel; (3) Meters per second; (4) Scale of speed.

In order to test the total static pressure at the inlet and outlet of the rotor, and parameters of steady-state conditions at the gas flow direction at the outlet of the rotor, a six-point total pressure probe is installed at the cross-sections of the inlet and outlet of the rotor. On the internal and external walls of the cross-section of the inlet and outlet, four static pressure holes are opened. At the cross-section of the rotor outlet, a single-point type total static pressure composite probe (capable of automatically tracking the direction of gas flow) is installed. The flow through the rotor is measured by using an inlet flow tube. The collection and recording of the steady-state parameters are done using an XJ-100 model automatic circulating detection and measurement instrument; some low-pressure parameters are directly read out with water discharge.

The measurements of dynamic-state parameters (under stall condition), the flow speed and total gas pressure are conducted

using a DISA/CTA series 55M model hot-wire anemometer and the sensor part of a Chinese-made LDY6-4 model pressure pulse instrument. The data collection and recording of the entire process of dynamic-state parameters are obtained by using a TEAC/R 510 model magnetic tape data recording instrument. In the entire testing process, the RS-1 model oscillograph was used to conduct on-site observation and monitoring of dynamic-state parameters. Refer to Literature [2] for the test method of dynamic-state parameters and data processing method.

III. Test Results and Analyses

1. The measured flow field and its analysis under rotating stall conditions of a transonic rotor

Refer to Fig. 3 for the basic-element stage measured flow field at the blade tip of a transonic rotor under rotating stall conditions. The flow field is the measured flow field with flow coefficient $\overline{C}_a$=0.263 and transonic rotor at 13,000 rpm. We can see from the flow field diagram that reverse flow zones exist before and after the cross-section of the rotor. The existence of the reverse flow zone will return the lower-stream gas after applying pressure and temperature increase by the rotor to the upper stream of the rotor. This is the main reason for burn corrosion of the compressor blades. The higher the supercharging ratio, the shorter is the time causing burn corrosion on blades by reverse flow; even this destruction phenomenon could occur within tens of seconds. For a rotor with axial-direction gas inlet, when reverse flow occurs, there are pre-rotation and vortex motions in the upper streams of the rotor. We can also obtain the following by comparing the low-speed rotor introduced in Literature [3] with the measured flow field: the reverse flow zone in the lower stream of the transonic rotor dissipates faster than the reverse flow zone of a low-speed rotor. In the flow field of a transonic rotor, the reverse flow zone in the lower stream of the rotor shrinks quite fast; no

reverse flow zone exists at cross-section IV about 170 mm from the rotor. However, the reverse flow zone in the lower stream of a low-speed rotor shrinks slowly, without dissipation until the channel exit. This situation explains why the vortex intensity in the transonic rotor attenuates more quickly than the vortex intensity in the low-speed rotor. In the flow field of rotating stall conditions of a transonic rotor, vortex motions exist in both the upper and lower streams of the rotor, and there is more attenuation of vortex intensity in the lower stream of the rotor; these facts play an important role in correcting and improving the theoretical flow model.

2. The onset, growth and cessation processes of rotating stall and its analysis

(1).Test resùlts and analysis at 8000 rpm

Figure 4 shows pressure signal oscillograms during the transition from the steady working condition to the stall condition. The measuring probe is installed at the blade tip 10 mm from the external hub. From the figure, fundamentally the mean value of the pressure signal does not vary in the transition process from steady to stall conditions. However, in the transient process, the amplitude of pulse oscillation of the pressure signal apparently increases. This mean pressure value before entering the rotating stall condition is fundamentally consistent with the mean pressure value of the steady-state condition; however, there is apparently the increasing flow phenomenon of the oscillation amplitude, termed in Literature [3] the phenomenon of turbulent separation. Figure 5 presents the pressure oscillograms of the amplified phenomenon of turbulent separation. We know from the figure that there are 17 pulses in the pressure oscillogram with each periodic range of a rotating speed. The rotational period is consistent with the /66
rotating period of the rotor in these 17 pulse zones. Since the number of blades of a rotor is 17, it provides a valid reason to

explain why the nature of the phenomenon of turbulent separation is a flow phenomenon of serious separation on each blade of the rotor before the rotor enters the rotating stall condition. Since the blade type is thin and slightly bent at the blade tip of the transonic rotor, this can further explain how a conclusion has been reached in studying the low-speed rotor where a relatively long duration of turbulent separation often appears before some basic-element stage (with a very small bending angle of blade type) enters the rotating stall condition; this conclusion also applies to a transonic rotor.

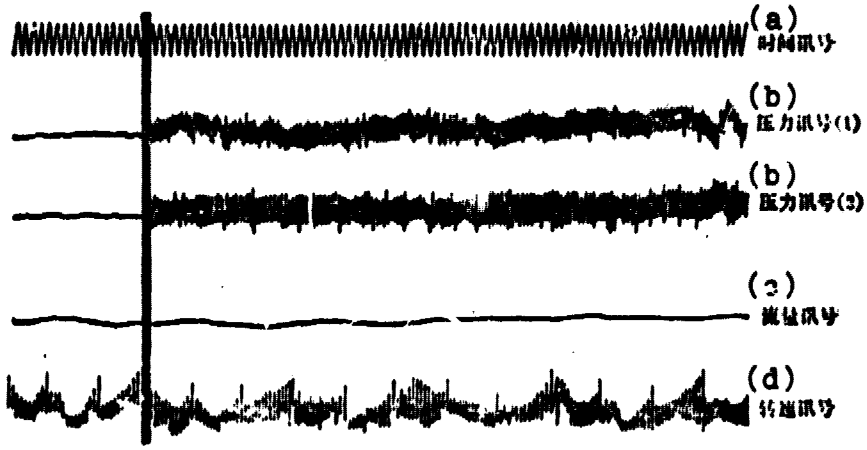

Fig. 4. The pressure signal oscillograms at n=8000 rpm in stall condition and in blade irregular separation condition.
Key: (a) Time signals; (b) Pressure signals; (c) Flow signals; (d) Signals of rotating speed.

While throttling from the condition of turbulent separation to the condition of rotating stall, the average value of the pressure signals apparently decreases, appearing as the rotating stall phenomenon in both zones. The rotating speed ($\bar{u}_{minute}=u_{minute}/u_{rotor}$) is 0.74. By throttling continuously, the number of separation zones changes from two to one but $\bar{u}_{minute}$ still remains 0.74. The working condition remains until the exhaust throttle valve is

at the completely closed position. At this rotating speed, no irregular oscillation appears in the compressor.

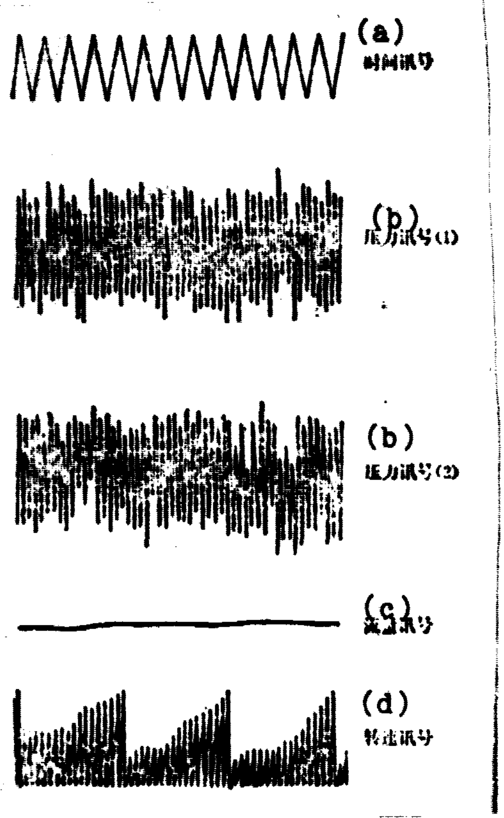

Fig. 5. The pressure signal oscillograms at n=8000 rpm in blade irregular separation condition.
Key: (a) Time signals; (b) Pressure signals; (c) Flow signals; (d) Signals of rotating speed.

(2). Experimental results and anallysis at 13,000 rpm

Two pressure probes are similarly installed at blade tips of the rotor. When the throttling valve is being closed with transition to the stall state, first the increasing longitudinal-direction pulse oscillation amplitude of the pressure oscillogram appears with a phenomenon of turbulent separation in serious separation on each blade (refer to the oscillogram in (1) of Fig. 6). Before onset of the rota- /67
ting stall, there is a new flow phenomenon of periodic variation on the mean value of a pulse type oscillation amplitude (refer to the oscillogram in (2) of Fig. 6). Since the variation period is the same as the period of one revolution of rotating speed, this is not the rotating stall, but a serious separation flow in the channal of each blade. In addition, this phenomenon further explains why there are different gas flows through the channel of each blade. The occurrence of this phenomenon is the prelude to the imminent rotating stall condition (refer to the transition between oscillograms of (2) and (3) in Fig. 6). This flow phe..nenon appearing before occurrence of the rota-

ting stall condition has not been included in past manuscripts; the variation process of the pressure oscillogram is shown in Fig. 6.

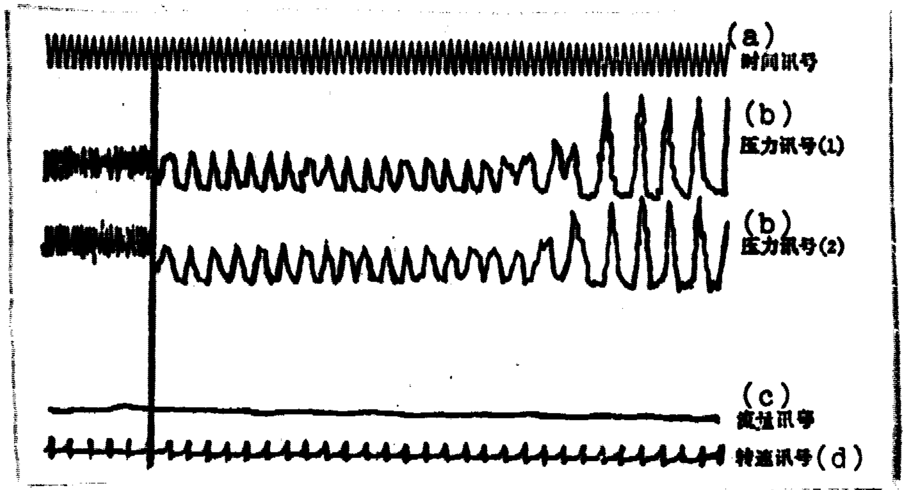

Fig. 6. The pressure signal oscillograms at n=13,000 rpm in blade irregular separation condition and in rotating stall condition: (1) Pressure signal oscillogram in blade irregular separation condition with similar mean value of amplitude; (2) Pressure signal oscillogram in blade irregular separation with amplitude mean value varying periodically; (3) Pressure signal oscillogram in rotating stall condition.
Key: (a) Time signals; (b) Pressure signals; (c) Flow signals; (d) Signals of rotating speed.

With continuous throttling after the appearance of the phenomenon of turbulent separation, a steady single-zone stall condition begins in sequence. The alternate appearance of the varying-state condition of the single-and-double zone and the steady condition of the double zone can lead to sequential appearance of a transient condition from the double zone toward the single zone and a steady single-zone condition. At last, the stall dissipates from the steady single-zone condition to the steady-state condition. Under the various stall conditions mentioned above, the rotating speed $\bar{u}_{minute}$ of the separation zone is about 0.7.

The oscillograms of hot-wire anemometer probes (Fig. 7) and pressure transducers (Fig. 8) are recorded under the transient state of a varying stall flow state. Two oscillograms in Fig. 8 are measured while two hot-wire anemometer probes are placed, respectively, at the blade tip and blade root of the rotor; the angle included between these two probes is also 90°. These four probes are placed on a single measurement cross-section. From Fig. 8, fundamentally the shape of both oscillograms is the same, with only a very small phase difference at the horizontal positions of the oscillograms. Very obviously, the horizontal distance is caused by the 90° difference in the included angle between the two probes in a circle. Now we analyze the variation of the two hot-wire oscillograms in Fig. 7: there is periodic variation of the width of the separation zone at the blade tip and blade root of the rotor; the variation period is considerably greater than the period of the rotor revolving speed. If the two oscillograms in the figure are moved in relation to each other by a period of one half width of the separation zone, we can see that the width of /68
separation zone at the blade root widens and the mean speed value becomes smaller; at the blade tip, the width of the separation zone is narrowed and the mean speed value becomes greater. The situation is just the same if vice versa. Therefore the width of the separation zone at the blade tip becomes, respectively, the narrowest and the widest when the width of the separation zone at the blade root reaches, respectively, the widest and the narrowest. By comprehensively analyzing the oscillograms obtained by two hot-wire anemometer probes at different blade heights as shown in Fig. 7, and the oscillograms obtained by two pressure probes placed at the blade tip as shown in Fig. 8, we can clearly see the following: in the transient state, the width of the separation zone varies not only periodically along the circumferential direction, but also has periodic wavy motion in the diametral direction of the blade. There is the same pulse frequency along the circumferential and the diametral directions, at about 18 Hertz. This

phenomenon may occur once the stall flow state of the rotor varies. It seems that this phenomenon explains the rotating stall condition; although the total flow remains constant as it passes a certain cross-section of the rotor, the flows of various basic-element stages may vary with time. The above flow phenomenon appears in the transonic rotor along the blade-height direction with relatively greater torsion on the blades; this phenomenon has not been reported in manuscripts either domestically or abroad. The discovery and proof of this phenomenon can provide a new and valuable force of excited oscillation by analyzing the forces acting on a blade. In addition, a new understanding of the configuration of unsteady flow may be obtained.

Fig. 7. The oscillograms measured by two hot-wire anemometer probes in the transient process of a rotating stall at n=13,000 rpm: the upper one--the probe located at the root of the blade; the lower one--the probe located at the tip of the blade. Key: (a) Time signals; (b) Hot-wire signals; (c) Flow signals; (d) Signals of rotating speed.

(3). Experimental results and analysis at 15,000 rpm /69

In the experimental and study process at 15,000 rpm, the measurement positions did not vary except that a hot-wire anemometer probe was placed at the middle of the blade instead of at the

original position at the blade tip of the rotor. The entire experimental process and the obtained conclusions are the same as for 13,000 rpm. We do not describe them here. This section only presents the oscillograms showing the speed value (refer to Fig. 9) obtained with two hot-wire probes in the variation process of the stall flow state.

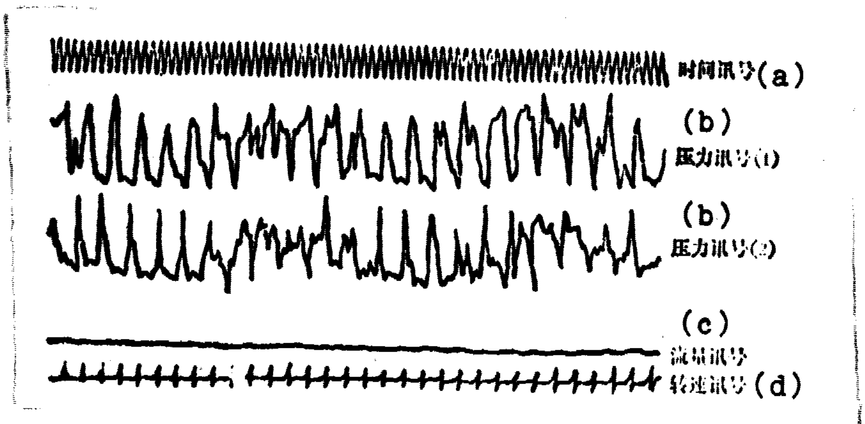

Fig. 8. The oscillograms measured by two pressure transducers in the transient process of a rotating stall at n=13,000 rpm (transducer located at the tip of the blade).
Key: (a) Time signals; (b) Pressure signals; (c) Flow signals; (d) Signals of rotating speed.

Conclusions

From this paper studying the rotating stall phenomenon of a transonic rotor, the following brief conclusions can be reached:

1. The vortex system flow model, using the vortex theory and established under the rotating stall condition, is sound. From calculation using the model, the obtained two-dimensional flow field matches quite well with the measured flow field.

2. From the measured flow field of a rotating stall condition obtained from transonic rotor experiments, we can see that reverse-

flow zones exist in the upper and lower streams of the rotor. This phenomenon explains the following: not only does the vortex motion exist in the lower stream of the rotor, it also exists in the upper stream. The reverse flow zone in the lower stream of the transonic rotor dissipates faster than the reverse flow zone of the low-speed rotor. This phenomenon explains that the dissipation of vortex intensity in the lower streams of the transonic rotor is faster than that in the low-speed rotor.

Fig. 9. The oscillograms measured by two hot-wire anemometer probes in the transient process of a rotating stall at n=15,000 rpm: the upper one--the probe located at the middle of the blade; the lower one--the probe located at the root of the blade. Key: (a) Time signals; (b) Hot-wire signals; (c) Flow signals; (d) Signals of rotating speed.

3. At the blade tip of the transonic rotor, the phenomenon of turbulent separation in the basic-element stages also occurs because the blades are relatively straight, pointed and thin. This phenomenon leads to the conclusion that a relatively longer time of turbulent separation often occurs before the basic-element stages (with a very small bending angle of the blade type) entering the rotating stall condition as reached in the study of the low-speed rotor.

4. In the rotating stall phenomenon occurring in some non-designed rpm of the transonic rotor, the relative rotating speed ($\bar{u}_{minute} = u_{minute}/u_{rotor}$) of the separation zone remains unchanged, about 70 percent of the rotor rpm. Therefore, the propagation speed of the separation zone relative to the blade row is 30 percent of the rotor rpm. This value is considerably lower than the propagation speed (50 to 60 percent of the rotor rpm) of the separation zone of the low-speed rotor. This phenomenon is possibly due to the effect of compressibility at the propagation speed of the relative blade row of the separation zone where there is the apparent intensifying effect in the transonic rotor.

5. In some non-designed rpm of transonic rotors, during the /70
dynamic-state process of varying the stall flow state, periodic variation with time may occur on the circumferential width of the separation zone. At the same time, periodic oscillation occurs along the diametral direction of the gas flow. The varying frequency of the period is 15 to 18 periods per second. After proof is obtained of this newly observed flow phenomenon, a new source of excited oscillation in analysis of forces acting on a blade becomes known. In addition, new understanding of the configuration of unsteady flow can be obtained.

These taking part in this experimentation were colleagues Feng Yucheng, Tao Deping, Li Baoju and Hu Zong'an, as well as Zhang Songchen, Zhang Suzhen, Liu Jiafeng and Hao Shucheng of Institute No. 606.

Submitted April 1981

REFEREMCES

(Reports)

1. Zhang Shunlin and Lu Yajun, "Flow Model under Rotating Stall Condition and the Calculating Method of the Flow Field," Research Report BH-B670 of the Beijing Aeronautical Engineering College, 1981, 7. (in Chinese)

2. Lu Yajun, Zhang Sunlin and Liu Jiafeng, "Experiments and Study of Rotating Stall Phenomenon in Transonic Rotor," Research Report BH-B669 of the Beijing Aeronautical Engineering College, 1981, 7. (in Chinese)

3. Lo Ya-tszyun': "Study of Rotating Stall (Effect of Impeller Cascade Characteristics)," Dissertation in Defense of Candidate of Technical Sciences Degree, 1963. (in Russian)

5. Day, I. J. and Cumpsty, N. A., "The Measurement and Interpretation of Flow within Rotating Stall Cell in Axial Compressors, " CUED/A-Turbo/TR90 1977.

(Journals)

4. Valensi, J., "Experimental Investigation of the Rotating Stall in a Single Stage Axial Compressor," Journal Aeronautical Science, Vol. 25, No. 1, 1958.